Applied Energy 225 (2018) 876–883

Contents lists available at ScienceDirect

Applied Energy

journal homepage: www.elsevier.com/locate/apenergy

Heterogeneity-assisted carbon dioxide storage in marine sediments

Zhenxue Dai[a,b,*], Ye Zhang[c], Jeffrey Bielicki[d,e], Mohammad Amin Amooie[f], Mingkan Zhang[c,g], Changbing Yang[h], Youqin Zou[i,j], William Ampomah[k], Ting Xiao[b,l], Wei Jia[l], Richard Middleton[b], Wen Zhang[a], Youhong Sun[a,*], Joachim Moortgat[f], Mohamad Reza Soltanian[m,*], Philip Stauffer[b]

[a] College of Construction Engineering, Jilin University, Changchun 130026, China
[b] Los Alamos National Laboratory, Los Alamos, NM, USA
[c] Department of Geology and Geophysics, University of Wyoming, Laramie, WY 82071, USA
[d] Department of Civil, Environmental, and Geodetic Engineering, The Ohio State University, Columbus, OH 43210, USA
[e] John Glenn College of Public Affairs, The Ohio State University, Columbus, OH 43210, USA
[f] School of Earth Sciences, The Ohio State University, Columbus, OH 43210, USA
[g] Energy & Transportation Science Division, Oak Ridge National Laboratory, TN 37831, USA
[h] Edwards Aquifer Authority, 900 E. Quincy St., San Antonio, TX 78215, USA
[i] Bureau of Economic Geology, The University of Texas at Austin, TX 78713, USA
[j] School of Resources, Environmental and Chemical Engineering, Nanchang University, Nanchang 330031, China
[k] Petroleum Recovery Research Center, New Mexico Tech, Socorro, NM 87801, USA
[l] Energy and Geoscience Institute, The University of Utah, Salt Lake City, UT 84108, USA
[m] Department of Geology, University of Cincinnati, Cincinnati, OH 45221, USA

HIGHLIGHTS

- CO_2 storage in heterogeneous marine sediments in investigated for the first time.
- CO_2 storage is possible in shallower marine sediments than previously found.
- Physical and operational thresholds for secure CO_2 storage are presented.

ARTICLE INFO

Keywords:
CO_2 storage
Marine sediment
Heterogeneity-assisted trapping

ABSTRACT

Global climate change is a pressing problem caused by the accumulation of anthropogenic greenhouse gas emissions in the atmosphere. Carbon dioxide (CO_2) capture and storage is a promising component of a portfolio of options to stabilize atmospheric CO_2 concentrations. Meaningful capture and storage requires the permanent isolation of enormous amounts of CO_2 away from the atmosphere. We investigate the effectiveness of heterogeneity-induced trapping mechanism, in potential synergy with a self-sealing gravitational trapping mechanism, for secure CO_2 storage in marine sediments. We conduct the first comprehensive study on heterogeneous marine sediments with various thicknesses at various ocean depths. Prior studies of gravitational trapping have assumed homogeneous (deep-sea) sediments, but numerous studies suggest reservoir heterogeneity may enhance CO_2 trapping. Heterogeneity can deter the upward migration of CO_2 and prevent leakage through the seafloor into the seawater. Using geostatistically-based Monte Carlo simulations of CO_2 transport in heterogeneous sediment, we show that strong spatial variability in permeability is a dominant physical mechanism for secure CO_2 storage in marine sediments below 1.2 km water depth (less than half of the depth needed for the gravitational trapping). We identify thresholds for sediment thickness, mean permeability and porosity, and their relationships to meaningful injection rates. Our results for the U.S. Gulf of Mexico suggest that heterogeneity-assisted trapping has a greater areal extent with more than three times the CO_2 storage capacity for secure offshore CO_2 storage than with gravitational trapping. These characteristics offer CO_2 storage opportunities that are closer to coasts, more accessible, and likely to be less costly.

* Corresponding authors at: College of Construction Engineering, Jilin University, Changchun130026, China. (Z. Dai)
E-mail addresses: dzx@jlu.edu.cn (Z. Dai), syh@jlu.edu.cn (Y. Sun), soltanma@ucmail.uc.edu (M.R. Soltanian).

https://doi.org/10.1016/j.apenergy.2018.05.038
Received 16 January 2018; Received in revised form 16 April 2018; Accepted 6 May 2018
Available online 26 May 2018
0306-2619/ © 2018 Elsevier Ltd. All rights reserved.

1. Introduction

Carbon dioxide (CO_2) capture and storage (CCS) can help stabilizing greenhouse gas concentrations in the atmosphere and mitigate global climate change [1–7]. Multiple approaches have been proposed for the long-term storage of anthropogenic CO_2 emissions, including injection into deep geologic formations (e.g., depleted oil and gas reservoirs, coalbeds, saline formations, shale [8–16]), deep ocean waters [17,18], and storage via chemical transformations [19,20]. However, each of these options has drawbacks. In onshore geologic formations, CO_2 is buoyant and can leak from the reservoir through an overlying impervious formation [21,22], and overpressure due to CO_2 injection may fracture the overlying caprock or induce seismicity [23,24].

Deep ocean waters may be acidified by CO_2, with concomitant impacts on marine ecosystems, and the CO_2 is prone to mixing with ocean currents and may be ultimately released to the atmosphere [25]. Further, industrial demand for chemical transformations is ~200 $MtCO_2$ per year, which is roughly 175 times less than the amount of CO_2 that was emitted from energy use worldwide in 2013 [22]. Offshore geologic formations could also be used for CO_2 storage, which may be beneficial because they are not beneath onshore populations, cannot negatively affect underground sources of drinking water [26], and regulatory considerations and ownership issues may be more easily reconciled than for onshore locations [27]. In fact, several offshore CO_2 storage projects are underway, including CO_2ReMoVe [28], SUCCESS [29], QICS [30], and NLECI [31], and NCIP [32]. Most of these projects are implemented in aquifers under shallow seas and, as in onshore geologic formations, there are hazards that arise from overpressure and the buoyancy of emplaced CO_2, such as, CO_2 interaction with seawater.

We revisit in detail a more promising option for CO_2 storage: emplacement in deep marine sediments [33–35]. CO_2 storage in deep marine sediments has the advantages of geologic storage and deep ocean storage [33]. For example, CO_2 storage in marine sediments can benefit from continuous subsea pressure management and potential chemical transformations through the formation of CO_2 hydrates [34]. While the costs are likely to be higher, CO_2 storage in marine sediments could be more tenable than other options for CO_2 storage, especially when risks are considered. We note that the cost evaluation and cost comparison to onshore CO_2 storage are outside the scope of our work.

At sufficient ocean depths, the pressure is high enough and the temperature is low enough for liquid CO_2 ($CO_{2(l)}$) to be more dense than the surrounding less compressible seawater [36]. If CO_2 was injected above the seafloor, it would sink and form a lake of gravitationally stable $CO_{2(l)}$ on the seafloor. But if CO_2 was injected into the sediments below the seafloor, the emplaced $CO_{2(l)}$ would descend deeper into the sediment. As it descends, the increase in temperature due to the geothermal gradient would cause the density of the $CO_{2(l)}$ to pronouncedly decrease. At the neutral buoyancy depth (NBD) into the sediments, the $CO_{2(l)}$ would stop descending because its density becomes equal to the density of the surrounding pore fluid, and thus the $CO_{2(l)}$ isolates itself within the sediment pores. Gravitational trapping occurs in the "negative buoyancy zone" [33] in marine sediments, located between the seafloor and the NBD, where the emplaced CO_2 is more dense than the pore fluid. This gravitational trapping exists at water depths >~2.5 km and sediments within several hundred meters beneath the seafloor [37]. Also, if CO_2 were injected beneath the NBD, it would ascend until it reaches the NBD, where it would then be gravitationally trapped.

Despite the advantages of CO_2 storage in marine sediments, the suitability of this option is poorly understood, and thus the global storage capacity, while potentially enormous, is highly uncertain [35,38]. Prior studies of CO_2 storage via gravitational trapping have assumed *homogeneous* sediments [33,35], but experimental, numerical, and field studies suggest that reservoir permeability heterogeneity may enhance CO_2 trapping by hindering the upward migration of buoyant CO_2 [39]. As such, models that incorporate permeability heterogeneity more accurately account for CO_2 fate and transport in the reservoir [40,41].

In this work, we perform reservoir simulations of CO_2 injection and its interaction with sediment pore water, based on fluid and sediment data from four sites in the U.S. Gulf of Mexico (GOM), shown in Fig. 1(a). The marine sediments at these sites are sufficiently thick and permeable for CO_2 storage. The sediment porosity and permeability have variable degrees of heterogeneity and anisotropy, which reflect the original and post-depositional processes [42–44]. We incorporate these heterogeneities and anisotropies at the reservoir level into our models, where we explicitly model solubility and gravitational trapping processes. Given the various temperatures and pressures in the marine sediments, and the uncertainty in fluid flow parameters, we develop and implement a statistical framework to quantify the uncertainty in CO_2 storage capacity and leakage into the seawater during the heterogeneity-assisted trapping of CO_2 in marine sediments. To best of our knowledge, this work is the first numerical simulation study on CO_2 sequestration in heterogeneous marine sediments.

We find a large CO_2 storage potential due to heterogeneity-induced trapping, which is also effective in combination with gravitational trapping for physico-gravitational trapping (PGT). Marine sediment reservoirs must also accommodate sufficient CO_2 injection rates, which under homogeneous permeability conditions also requires that the sediments be thick and permeable, but such characters are uncommon in most deep-water settings [34,35]. We further show that these constraints can be relaxed through heterogeneity-induced trapping, such that marine sediments in much shallower seas can be viable CO_2 storage options.

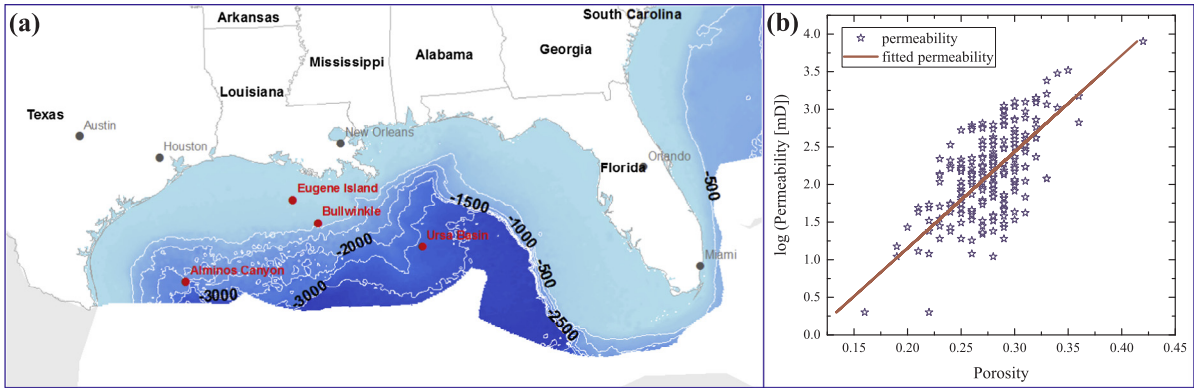

Fig. 1. Data from the Gulf of Mexico (GOM) within the U.S. Exclusive Economic Zone. (a) Site locations in the Gulf of Mexico (GOM), (b) Permeability-porosity correlations.

Table 1
Parameters for Base Cases and for the distributions used in Monte Carlo (MC) simulations of CO_2 storage in the GOM sediments.

Sediment Properties	Base Case	Sampling Characteristics		
		Min.	Max.	Distribution
Sediment thickness b (m)	500	5	900	Uniform
Mean permeability k (D)	1	0.001	8	Log Uniform
Anisotropy factor	0.1	0.01	0.5	Uniform
Log permeability variance	1.0	0.0	5.0	Uniform
Horizontal integral scale (km)	1.0	0.5	5.0	Uniform
Mean porosity, ϕ	0.2	0.1	0.42	Correlated to k (Eq. (1))
Physical Properties				
Water depth, d (km)	2.5	0.1	4.4	Uniform
CO_2 injection rate (kg/s)	0.3	0.002	2.0	Uniform
Seafloor temperature T_{sf} [°C]	2	1	20	Correlated to d (Eq. (2))
Geothermal gradient G (°C/km)	20	5	50	Correlated to d (Eq. (3))

2. Materials and methods

2.1. Characteristics of the Gulf of Mexico (GOM) Sites

We chose sediment and fluid data from four sites located in GOM (see Fig. 1(a)). Several investigations into marine sediments have been conducted at the four selected sites [42]. At the Alminos Canyon site, the Oligocene sediments have high porosity (0.28–0.34) and permeability (0.1–3 D) [43]. At Bullwinkle, sediments mainly contain interconnected sheet and channel sands with an average porosity and permeability of 0.33 and 2.4 D, respectively. In the Ursa Basin, horizontal permeability of the Ursa Siltstone is estimated at around 0.001 D [42], while the corresponding vertical permeability is about one to two orders of magnitude smaller. At the Eugene Island site, a thick sequence of shale is overlain by increasingly sand-rich sediments. Laboratory core measurements yield a range of permeabilities from 0.0002 to 8 D, while the corresponding porosities range from 0.16 to 0.35 [44]. Using permeability and porosity data form the sites, we developed a first-order log-linear relationship between porosity and horizontal permeability based on data from these four sites (Fig. 1(b)):

$$\phi = 0.11 + 0.078 log_{10} k \quad (1)$$

where ϕ is porosity and k is horizontal permeability. Eq. (1) and the estimated coefficients are used to populate the reservoir models with petrophysical properties that represent the GOM sediments. Studies of the geothermal features of the northwestern GOM continental slope provide approximate relation between water depth (d [m]) and seafloor temperature (T_{sf}) [45]:

$$T_{sf}\,[°C] = 295.1 d^{-0.6} \quad (2)$$

and a relation between the water depth and geothermal gradient (G) is [45]:

$$G\,[°C/km] = -9.6 ln(d) + 88.4. \quad (3)$$

Among the uncertain sediment characteristics, the vertical spatial integral scale of log-permeability was estimated from logging data and varies from 5 to 50 m. Assuming a fixed statistical anisotropy ratio of 100 between horizontal and vertical integral scales, the horizontal integral scale thus varies from 0.5 to 5.0 km. The permeability anisotropy factor (ratio of vertical to horizontal permeability) was also varied to reflect the possible existence of small-scale sedimentary stratification. The log-permeability variance was assumed to range from 0.0 (i.e., homogeneous) to 5 (i.e., highly-heterogeneous). The side boundaries are no-flow boundaries and the top boundary is open to flow. The van Genuchten model with appropriate coefficients for sediments was used for relative permeability functions in the CO_2-water multiphase flow simulations [46]. The liquid CO_2 diffusion coefficient is 10^{-9} m^2/s [47,48]. The numerical simulations were conducted with a finite element multiphase flow simulator, FEHM [49].

2.2. Base cases to demonstrate gravitational and heterogeneity-induced trapping

The Homogeneous Sediment Base Case demonstrates gravitational trapping by representing homogeneous sediments with permeability of 1 D and vertical permeability of 0.1 D. The Heterogeneous Sediment Base Case demonstrates heterogeneity-induced gravitational trapping by representing heterogeneous sediment permeability, where distributions are generated with Sequential Gaussian Simulation with mean permeability of 1 D, log-permeability variance of 1.0, and horizontal and vertical log-permeability integral scales of 1.0 and 0.1 km, respectively. Porosity is computed from horizontal permeability by Eq. (1). Both Base Cases use a 1 °C seafloor temperature at a depth consistent with prior findings of gravitational trapping (~2.5 km) [33,35], and a maximum estimated geothermal gradient in the GOM for depths greater than 1.2 km (20 °C/km). In both cases, the marine sediment reservoir is modeled with a two-dimensional (2D) cross-section with 500 m thickness, 5000 m width, and a lateral length of unity. The domain size was chosen based on our initial modeling test to make sure that the domain is large and wide enough to encompass the scale of heterogeneity, the lateral boundaries do not impact the temporal dynamic of CO_2 transport, and numerical simulations are practically efficient. The other parameters are provided in Table 1. CO_2 injection is simulated at a rate of 0.3 kg/s into the bottom-center of the reservoir for ten years (94,608 metric tonnes CO_2), after which CO_2 transport is simulated for 200 years.

2.3. Statistical framework to characterize heterogeneities

We developed and implemented a statistical framework to characterize heterogeneities, and to determine the effectiveness of the trapping mechanisms in the marine sediments with respect to uncertainties in six key parameters in Table 1 including water depth, sediment thickness, porosity, mean permeability, log-permeability variance, and injection rate. As in most offshore settings, univariate statistics and spatial distributions of these parameters are uncertain for the GOM because data are obtained from a few locations. To generate statistical distributions that can be used to quantify the uncertainty ranges, we used available data from four sites in the GOM (Fig. 1(a)): Alminos Canyon, Bullwinkle, Ursa Basin, and Eugene Island.

We performed sets of Monte Carlo (MC) simulations using the distributions determined for each key parameter. Other input parameters are the same as those in the Heterogeneous Sediments Base Case. Each set of MC simulations is comprised of 100 samples and uses our computationally efficient statistical framework [50]. In each of the MC simulations, PGT is assessed through the normalized rate of CO_2 leakage from the sediment to the seafloor, which is calculated as the percentage-by-mass of the injected CO_2 that leaks out from the top of the model.

2.4. Monte Carlo simulations

We used Latin Hypercube in the MC simulations to sample the uncertain input parameters and to build 1000 geostatistically-based realizations [51]. Permeability and porosity fields of each realization are generated with Sequential Gauss Simulation in GEOST [52]. To reflect sediments in near-shore to deep-water environments, the water depth was varied from 0.1 to 4.4 km, and we used Eq. (2) and Eq. (3) to determine the distributions of seafloor temperature and geothermal gradient. For a given sediment thickness sampled from its distribution, the dimensions of the model and its discretization were obtained automatically.

2.5. Global sensitivity analysis

We applied a computationally efficient global sensitivity analysis technique, based on multivariate adaptive regression spline (MARS) [51], to investigate the sensitivities of CO_2 leakage rate to variations in the input parameters. The MARS technique is based on computations of the variance of conditional expectation (VCE) of an output variable (Y):

$$\mathrm{VCE}(X_k) = \frac{1}{s}\sum_{j=1}^{s}(\overline{Y}_j - \overline{Y})^2 - \frac{1}{sr^2}\sum_{j=1}^{s}\sum_{i=1}^{r}(Y_{ij} - \overline{Y}_j)^2, \quad (4)$$

where VCE quantifies the variability in the conditional expected values of Y when an uncertain input parameter (X_k) varies in the entire parameter space. For X_k,s is the number of distinct values sampled from its distribution, and r is the number of replications. $N = sr$ is the sample size. We used Eq. (4) to quantify and rank the sensitivities of Y to the key input parameters.

2.6. Estimated CO_2 storage capacity in the GOM

We used Eq. (2) on bathymetry data to estimate seafloor temperature ($T_{sf,i}$) (Fig. 2(a)) and geothermal gradient (G) (Fig. 2(b)) for seafloor depth of d_i at each location, i, within the U.S. Exclusive Economic Zone. The temperature at depth b_i in the sediment, $T_{b,i}$, was calculated as $T_{b,i} = T_{sf,i} + b_i G$, and the pressure was calculated as $P_{b,i} = \Delta P(d_i + b_i)$ with constant hydrostatic pressure gradient (ΔP) of 10.5 MPa/km. To determine b_i, we used data on the thickness (t_i) of the sediment at each location [53]. We assumed that PGT occurs in 500 m of sediment, and estimated $T_{b,i}$ and $P_{b,i}$ at the midpoint of this column, b_i = 250 m, which implicitly assumes that the change in density in the sediment is a linear function of depth. We established Eq. (5) for the density of CO_2,ρ_{CO_2}, by regressing data over these ranges of $T_{b,i}$ and $P_{b,i}$ [54].

$$\begin{aligned}\rho_{CO_2,i} = {} & 936.72 - 2.8194(T_{b,i} - T_0) - 0.0004801(T_{b,i} - T_0)^2 \\ & + 0.0000234(T_{b,i} - T_0)^3 + 3.6318(P_{b,i} - P_0) \\ & - 0.052229(P_{b,i} - P_0)^2 + 0.0009794(P_{b,i} - P_0)^3 \\ & + 0.03842(T_{b,i} - T_0)(P_{b,i} - P_0) - 0.0008558(T_{b,i} - T_0)(P_{b,i} - P_0)^2 \\ & + 0.0001023(T_{b,i} - T_0)^2(P_{b,i} - P_0), \end{aligned} \quad (5)$$

where T_0 = 335 K and P_0= 52 MPa. We estimated the density of CO_2 at b_i and multiplied the results by the data in Fig. 3(f), which shows that emplaced CO_2 exists in a column from the seafloor to a depth of approximately two-thirds of the sediment thickness ($2/3b_i$). We then assigned a 20% porosity and assumed that 2/3 of the area for each threshold depth was comprised of low-permeability rocks (log-permeability < -14). As such, our capacity estimates are applicable to 1/3 of the areas within the GOM.

3. Results

3.1. Gravitational and heterogeneity-induced trapping

We present the results of Base Cases for CO_2 injection into homogeneous and heterogeneous marine sediments before presenting results from our statistical characterization of heterogeneities and the dependence of key CO_2 storage parameters on these heterogeneities. Our results for these Base Cases are shown in Fig. 3 (left and right panels correspond to Homogeneous Base Case and Heterogeneous Base Case, respectively). In the Homogeneous Sediments Base Case, the upward migration of $CO_{2(l)}$ is axisymmetrically uniform around the injection point. Further upward migration is impeded by the negatively buoyant $CO_{2(l)}$ above the NBD (Fig. 3(a) and (b)). Gravitational trapping in marine sediments is thus manifest by stratified layers of: (*i*) pore fluid below the seafloor, (*ii*) higher density $CO_{2(l)}$ below this pore fluid and above the NBD, and (*iii*) lower density $CO_{2(l)}$ that is ascending from below. The pore fluid serves as a top buoyancy cap for higher density $CO_{2(l)}$, which together act as a buoyancy cap for the lower density $CO_{2(l)}$ in turn. During our 200 years simulation, the estimated CO_2 leakage from the top of the sediment into the sea is ~0.1% of the total injected CO_2. In the Heterogeneous Sediments Base Case, the sparsely-distributed, low-permeability layers (dark blue[1] in Fig. 3(h)) hinder the upward migration of $CO_{2(l)}$. In contrast to the results for the Homogeneous Sediments Base Case, the $CO_{2(l)}$ in heterogeneous sediments does not reach the seafloor and there is no CO_2 leakage into the seawater during the 200-year simulation period (Fig. 3(e) and (f)). In addition to hindering the migration of emplaced $CO_{2(l)}$, sediment heterogeneity results in non-uniform temperatures and temperature gradients within the reservoir. This spatially thermal heterogeneity results from differences in thermal conductivities and specific heats between the sediment and the pore fluid, and produces spatially non-uniform profiles of $CO_{2(l)}$ density. For example, relative to homogeneous sediments at the same depth, the density of the $CO_{2(l)}$ is lower in high permeability layers that are overlain by low permeability layers in heterogeneous sediments. In both Base Cases, less than 5% of the total emplaced CO_2 is stored by dissolution process, and the rest is stored by gravitational and heterogeneity-assisted trapping mechanisms.

3.2. Sediment heterogeneity and threshold water depth

The synergy between gravitational trapping and heterogeneity-induced trapping in the Base Cases suggests that deep marine sediments have a much larger, and more secure, storage potential than has been previously identified. We sampled water depth with one set of Monte Carlo (MC) simulations for each of three values for the variance of log-permeability to represent various degrees of sediment heterogeneity: (1) 0.0 (homogeneous), (2) 1.0 (weakly-heterogeneous), and (3) 5.0 (strongly-heterogeneous). Our result for homogeneous sediments is consistent with prior work (e.g., [33]) in which gravitational trapping occurs in >2.5 km deep water. However, for shallow water depth of 0.5 km about 80% CO_2 leaks in homogeneous case. But sediment heterogeneity affects CO_2 transport such that secure CO_2 storage occurs with heterogeneity-induced trapping in sediments in shallower seas: >2.0 km for the weakly-heterogeneous sediments, and >1.2 km for the strongly-heterogeneous sediments (Fig. 4(a)). In strongly heterogeneous case with shallow water depth of 0.5 km about 30% of the injected CO_2 leaks through the seafloor. Therefore, careful consideration is needed in shallower depth even in highly heterogeneous case.

3.3. Injection rate and threshold sediment thickness and mean permeability

We investigated the effect of three injection rates (0.2, 0.02, and 0.002 $kgCO_2/s$) in weakly-heterogeneous sediments and water depth of 2.5 km by sampling sediment thickness and mean permeability for each injection rate. A total of six sets of MC simulations were conducted. In the reservoir model with 1 m lateral length, PGT occurs when the sediment is >400 m thick for an injection rate of 0.2 $kgCO_2/s$, >210 m thick for a 0.02 $kgCO_2/s$, and >90 m thick for an injection rate of 0.002 $kgCO_2/s$ (Fig. 4(b)). As the injection rate increases, the sediments must be thicker to accommodate the CO_2 that accumulates on either side of the NBD. Our results suggest that the threshold sediment thickness for PGT roughly doubles for every order of magnitude increase in the injection rate.

As shown in Fig. 4(c), PGT occurs when the mean permeability is > 10^{-14} m^2 for an injection rate of 0.2 $kgCO_2/s$, and at a smaller mean permeabilities (~10^{-15} m^2) for the lower injection rates. Since porosity is positively correlated with permeability (see Eq. (1) in the Materials and Methods section), the corresponding minimum mean porosities are

[1] For interpretation of color in Fig. 3, the reader is referred to the web version of this article.

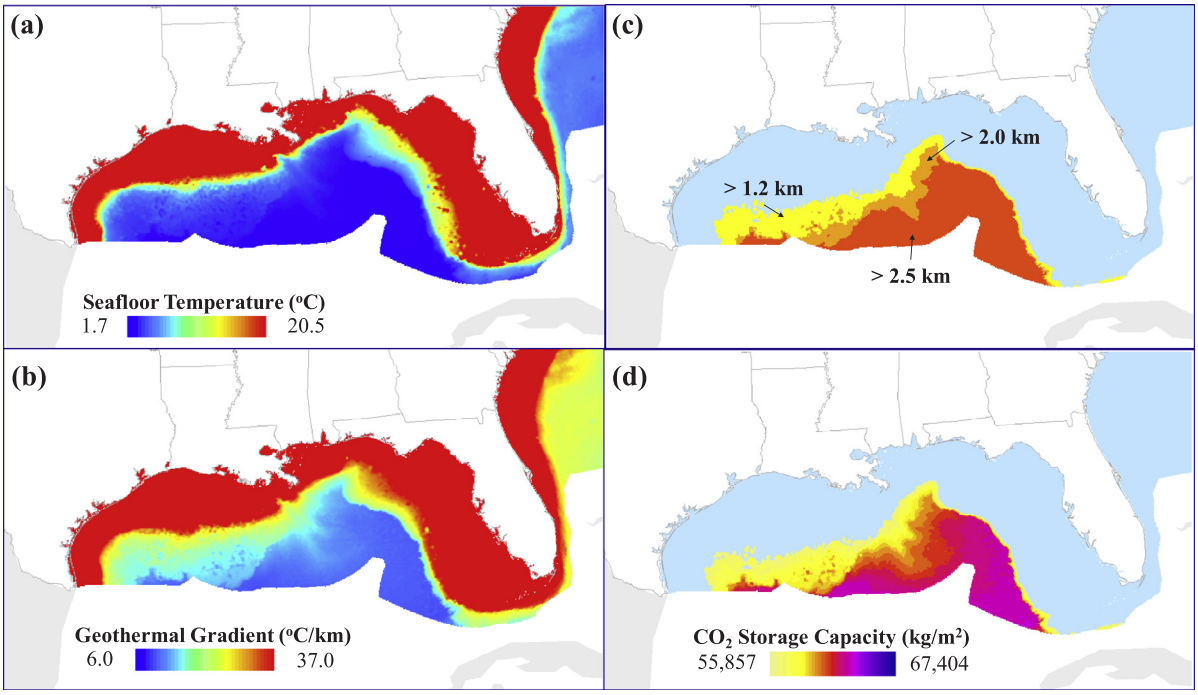

Fig. 2. Data from the Gulf of Mexico (GOM) within the U.S. Exclusive Economic Zone. (a) Estimated seafloor temperature, (b) Estimated geothermal gradient, (c) Areas encompassing threshold depths for physico-gravitational trapping (PGT) in sediments with strong heterogeneity (1.2 km), weak heterogeneity (2.0 km), and no heterogeneity (2.5 km), and (d) Estimated CO_2 storage capacity in the marine sediments.

0.18 (for 0.2 $kgCO_2/s$), and 0.10 (for 0.02, and 0.002 $kgCO_2/s$). These results suggest that a minimum mean permeability and mean porosity are necessary for secure CO_2 storage in marine sediments, and more CO_2 can be stored with higher permeabilities and porosities.

3.4. Sensitivity to injection rate

Using the parameters for the Heterogeneous Sediments Base Case, we sampled the CO_2 injection rate in one set of MC simulations. PGT occurs for injection rates below 0.325 $kgCO_2/s$ (Fig. 4(d)). The CO_2 injectivity in three dimensions can be approximated by multiplying this threshold rate by a realistic lateral length for a reservoir. For example, in a reservoir with a 500 m lateral length, PGT occurs for a CO_2 injection rate below 162.5 kg of CO_2/s (~5 $MtCO_2/yr$) (close to the injection rate used in some CO_2 pilot projects such as Cranfield, Mississippi [13,55]). Moreover, the maximum injection rate that enables PGT increases in deeper water, thicker sediments, or higher mean permeabilities (and porosities). In the GOM, the Alminos Canyon and Ursa Basin sites are deeper than 2.0 km, and have sediments that are at least weakly-heterogeneous (log-permeability variance >1.0 in the data). As such, these sites may have the capacity for securely storing CO_2 in the marine sediments with PGT for high CO_2 injection rates.

3.5. Sensitivity analysis

We investigated the sensitivities of CO_2 leakage rate to variations in the input parameters (Table 1), as described in Section 2.5. Detailed global sensitivity analyses on the key, yet uncertain, CO_2 storage parameters in marine sediments are shown in Fig. 5. Our results reveal that PGT is most sensitive to (in decreasing order): permeability anisotropy, CO_2 injection rate, seawater depth, sediment thickness, variance in permeability, and mean permeability, followed by parameters that are correlated with some of these items: mean porosity (correlated with mean permeability), and seafloor temperature and seafloor pressure (both are correlated with depth). Larger permeability anisotropy has the strongest control on CO_2 leakage resulting in a faster CO_2 transport in vertical direction, which in turn, leads to higher CO_2 leakage. Higher CO_2 injection rate leads to faster CO_2 transport in both high and low permeability media resulting in higher rate of leakage.

4. Implications and concluding remarks

We investigated CO_2 storage in heterogeneous marine sediments as a function of several key, yet uncertain, parameters. We found that variance in sediment permeability and porosity deters CO_2 migration and leakage through the seafloor, and heterogeneity-induced trapping can be achieved in a marine sediments in sea depths of 1.2 km, which is roughly half the depth that is necessary for gravitational trapping. Heterogeneity-induced trapping can also enhance gravitational trapping at the depths where it occurs.

These results suggest the potential for substantial revisions to prior assessments of the resource potential for secure CO_2 storage. In the GOM alone, with homogeneous sediments the sea must be at least 2.5 km deep, and there are 133,440 km^2 in which a total of 2935.7 Gt of CO_2 can be stored by gravitational trapping. If the sediments are weakly heterogeneous, the marine sediment storage potential increases to more than 3734.2 Gt of CO_2 in the 169,738 km^2 of 2.0 km or deeper water (about 30% higher than the homogeneous case). Further, if the sediments are highly heterogeneous, an estimated 5437.8 Gt of CO_2 can be stored in marine sediments in the 244,702 km^2 with the sea depths greater than 1.2 km (about 85% and 46% higher than the homogeneous and weakly heterogeneous cases, respectively) (Table 2 and Fig. 2(e)). The ability of heterogeneous sediments to provide secure CO_2 storage increases the quantity of CO_2 that could be stored at a given location, and provides opportunities for CO_2 storage that are closer to the shore and many sources of CO_2. Our results also provide guidance for thresholds of important operational and physical parameters for planning and deploying CO_2 storage in marine sediments. As sediment heterogeneity increases, the threshold depth for heterogenity-induced trapping decreases. Higher injection rates require thicker sediments and higher mean permeabilities, but injection rates that are greater than those in existing onshore and offshore projects can be accommodated

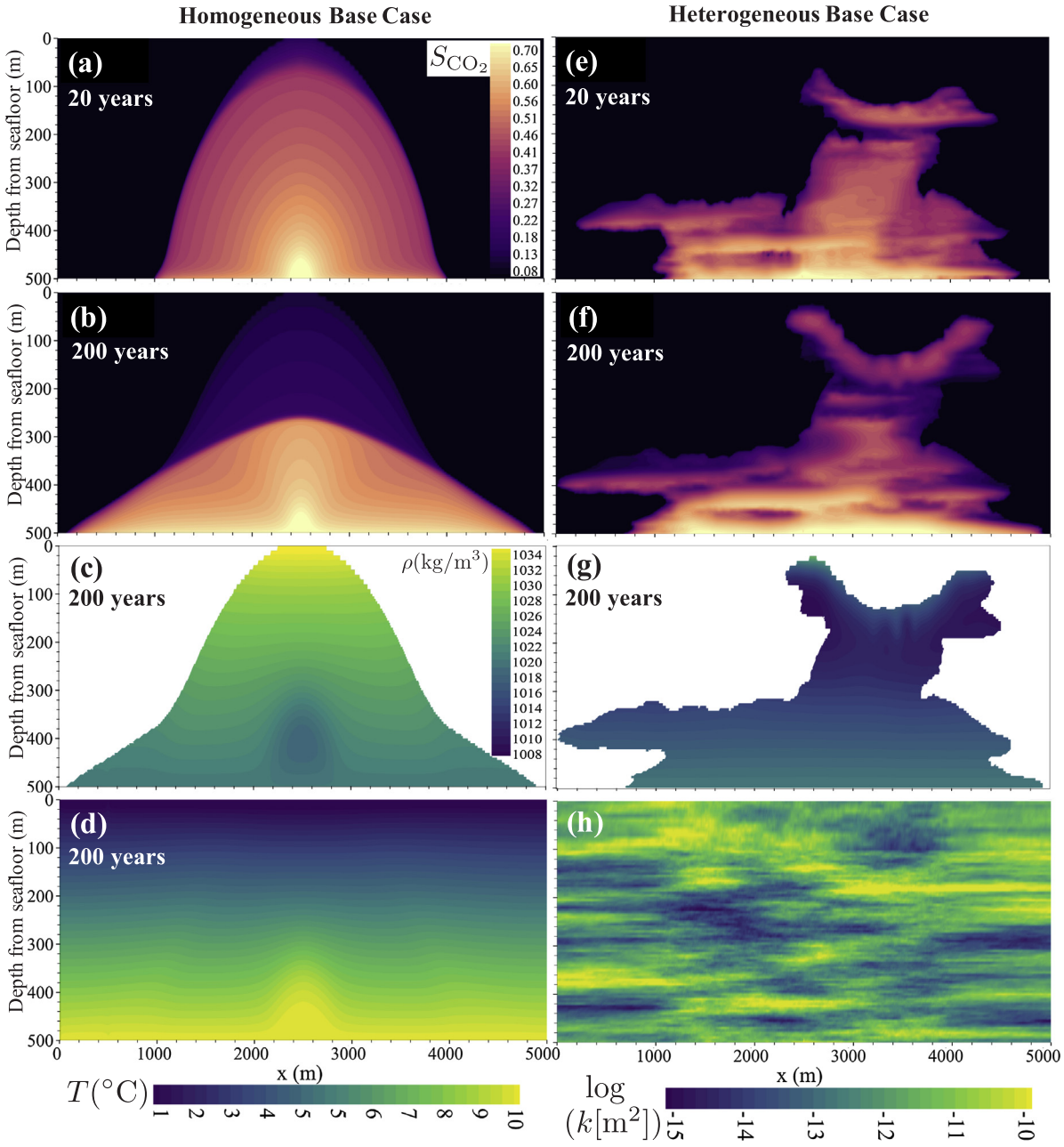

Fig. 3. Results for Bases Cases of sediment permeability under 2.5 km deep water: Homogeneous sediments (left 4 panels) with $CO_{2(l)}$ saturation at (a) 20 and (b) 200 years, (c) $CO_{2(l)}$ density, and (d) sediment temperature. Heterogeneous sediments (right 4 panels) with $CO_{2(l)}$ saturation at (e) 20 and (f) 200 years, (g) $CO_{2(l)}$ density, and (h) heterogeneous log-permeability field.

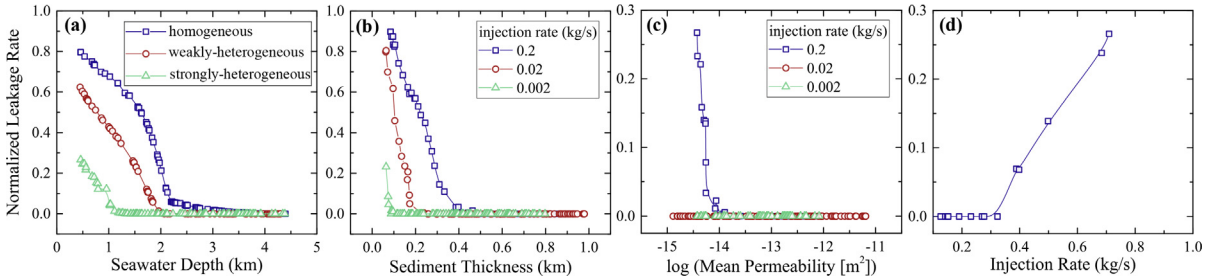

Fig. 4. Physico-Gravitational Trapping as indicated by Normalized Leakage Rate (percentage-by-mass of the injected $CO_{2(l)}$ that leaks out from the top of the model) from the sediment to the seawater. Effect of (a) seawater depth with variance of 0 representing the homogeneous case, (b) sediment thickness, (c) mean permeability, and (d) injection rate. Panels (b) to (c) show results for weakly heterogeneous sediment and water depth of 2.5 km.

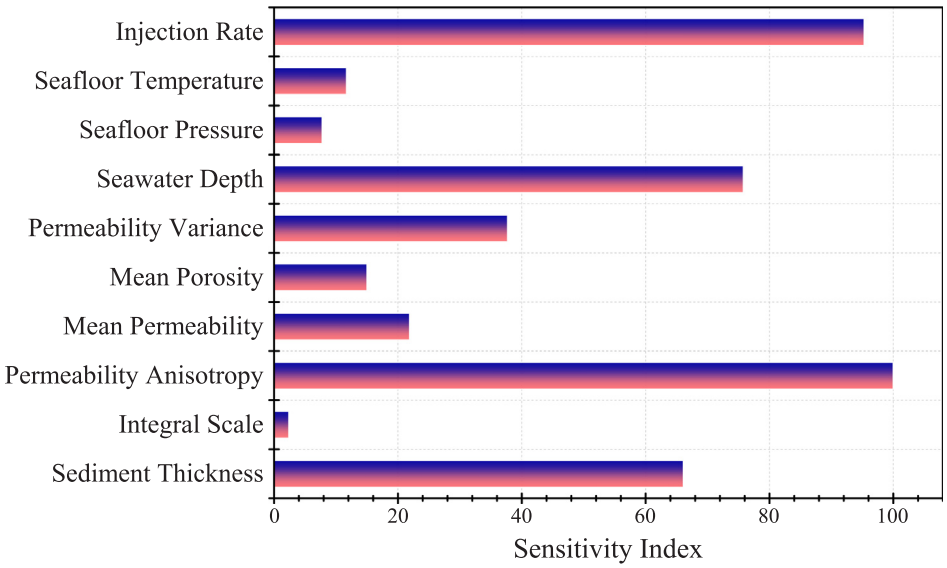

Fig. 5. The computed sensitivity index of the normalized CO_2 leakage rate (percentage-by-mass of the injected $CO_{2(l)}$ that leaks out from the top of the model) for each uncertain input parameter that was varied in the global sensitivity analysis.

Table 2
Summary of threshold values for Physico-Gravitational Trapping (PGT) in marine sediments (also see Fig. 2(c and d)).

	Log-permeability variance		
	0.0	1.0	5.0
Threshold depth (km)	>2.5	>2.0	>1.2
Storage area (km^2)	133,440	169,738	244,702
Storage capacity ($GtCO_2$)	2935.7	3734.2	5437.8
	CO_2 Injection Rate (kg/s)		
	0.2	0.02	0.002
Threshold sediment thickness (m)	>400	>210	>90
Threshold mean permeability (m^2)	$>10^{-14}$	$>10^{-15}$	$>10^{-15}$

by realistic mean permeabilities and reservoir sizes. Variations in seafloor depths and sediment thicknesses at actual locations where CO_2 storage in marine sediments may be deployed will also affect the amount of CO_2 that can be emplaced. For example, in our case study, the greatest estimated CO_2 storage capacity exists in the deeper water offshore of Florida, in the eastern GOM (Fig. 2(e) and (f)). Even though the sediments are thinner than in the other parts of the GOM, the higher density of the emplaced CO_2 results in higher estimated storage capacities. Other factors such as geomechanical and geochemical considerations, deformation due to CO_2 injection, and impacts of background flows are likely to revise the threshold water depths and estimated capacities for secure CO_2 storage in marine sediments with heterogeneity-induced and gravitational trapping mechanisms. We are, however, able to conclude that a far greater areal extent may be available for the secure offshore CO_2 storage than has been previously proposed, owing to the impact of sediment heterogeneity on CO_2 migration, and the likely reduction in overall costs associated with much shallower emplacement targets. We hope that our results provide optimism to develop future studies on CO_2 storage in marine sediments. We also hope that future laboratory and field scale data do become available that support self-sealing gravitational trapping mechanisms in marine sediments. There are certainly technologies that may provide more data about injected CO_2, and we hope that our work motivates their use in marine sediments. For instance, long-term deployment (years) of seismic tomography may be able to directly image the CO_2 plume in marine sediments in the future.

Acknowledgements

This work is partially funded by Jilin University through a start up project awarded to the first author and the National Natural Science Foundation of China [Grant numbers: 41772253]. Additional funding was provided by the US-China Clean Energy Research Center, Advanced Coal Technology Consortium directed by West Virginia University, and the U.S. National Science Foundation Sustainable Energy Pathways Program (1230691). We appreciate the constructive comments on the MC simulations provided by Rajesh Pawar, Peter Lichtner, and Hari Viswanathan.

References

[1] IPCC. Special report on carbon dioxide capture and storage. Cambridge, UK: Cambridge Univ Press; 2005.
[2] Szulczewski ML, MacMinn CW, Herzog HJ, Juanes R. Lifetime of carbon capture and storage as a climate-change mitigation technology. Proc Natl Acad Sci USA 2012;109(14):5185–9.
[3] Shaffer G. Long-term effectiveness and consequences of carbon dioxide sequestration. Nat Geosci 2010;3(7):464–7.
[4] Sharma SS. Determinants of carbon dioxide emissions: empirical evidence from 69 countries. Appl Energy 2011;88(1):376–82.
[5] Gunter W, Wong S, Cheel D, Sjostrom G. Large CO_2 sinks: Their role in the mitigation of greenhouse gases from an international, national (Canadian) and provincial (Alberta) perspective. Appl Energy 1998;61(4):209–27.
[6] Zhou W, Wang T, Yu Y, Chen D, Zhu B. Scenario analysis of CO_2 emissions from Chinas civil aviation industry through 2030. Appl Energy 2016;175:100–8.
[7] Viebahn P, Vallentin D, Höller S. Prospects of carbon capture and storage (ccs) in indias power sector–an integrated assessment. Appl Energy 2014;117:62–75.
[8] Jiang X. A review of physical modelling and numerical simulation of long-term geological storage of CO_2. Appl Energy 2011;88(11):3557–66.
[9] Nimana B, Canter C, Kumar A. Energy consumption and greenhouse gas emissions in the recovery and extraction of crude bitumen from canadas oil sands. Appl Energy 2015;143:189–99.
[10] Wang Z, Wang J, Lan C, He I, Ko V, Ryan D, et al. A study on the impact of SO_2 on CO_2 injectivity for CO_2 storage in a canadian saline aquifer. Appl Energy 2016;184:329–36.
[11] Tapia JFD, Lee J-Y, Ooi RE, Foo DC, Tan RR. Optimal CO_2 allocation and scheduling in enhanced oil recovery (eor) operations. Appl Energy 2016;184:337–45.
[12] Soltanian MR, Amooie MA, Dai Z, Cole D, Moortgat J. Critical dynamics of gravito-convective mixing in geological carbon sequestration. Sci Rep 2016;6:35921.
[13] Soltanian MR, Amooie MA, Cole DR, Graham DE, Hosseini SA, Hovorka S, Pfiffner SM, Phelps TJ, Moortgat J, et al. Simulating the Cranfield geological carbon sequestration project with high-resolution static models and an accurate equation of state. Int J Greenh Gas Control 2016;54:282–96.
[14] Ampomah W, Balch R, Cather M, Will R, Gunda D, Dai Z, et al. Optimum design of CO_2 storage and oil recovery under geological uncertainty. Appl Energy 2017;195:80–92.
[15] Welkenhuysen K, Rupert J, Compernolle T, Ramirez A, Swennen R, Piessens K.

Considering economic and geological uncertainty in the simulation of realistic investment decisions for CO_2-EOR projects in the north sea. Appl Energy 2017;185:745–61.
[16] Kim Y, Jang H, Kim J, Lee J. Prediction of storage efficiency on CO_2 sequestration in deep saline aquifers using artificial neural network. Appl Energy 2017;185:916–28.
[17] Haugan PM, Drange H. Sequestration of CO_2 in the deep ocean by shallow injection. Nature 1992;357(6376):318–20.
[18] Song J, Zhang D. Comprehensive review of caprock-sealing mechanisms for geologic carbon sequestration. Environ Sci Technol 2012;47(1):9–22.
[19] Lackner KS. Carbonate chemistry for sequestering fossil carbon. Annu Rev Energy Environ 2002;27(1):193–232.
[20] Ola O, Maroto-Valer MM, Mackintosh S. Turning CO_2 into Valuable Chemicals. Energy Proc 2013;37:6704–9.
[21] Bielicki JM, Pollak MF, Fitts JP, Peters CA, Wilson EJ. Causes and financial consequences of geologic CO_2 storage reservoir leakage and interference with other subsurface resources. Int J Greenh Gas Control 2014;20:272–84.
[22] Bielicki JM, Pollak MF, Deng H, Wilson EJ, Fitts JP, Peters CA. The leakage risk monetization model for geologic CO_2 storage. Environ Sci Technol 2016;50(10):4923–31.
[23] Zoback MD, Gorelick SM. Earthquake triggering and large-scale geologic storage of carbon dioxide. Proc Natl Acad Sci USA 2012;109(26):10164–8.
[24] Vilarrasa V, Carrera J. Geologic carbon storage is unlikely to trigger large earthquakes and reactivate faults through which CO_2 could leak. Proc Natl Acad Sci USA 2015;112(19):5938–43.
[25] Jain AK, Cao L. Assessing the effectiveness of direct injection for ocean carbon sequestration under the influence of climate change. Geophys Res Lett 32 (9).
[26] Eccles JK, Pratson L. Economic evaluation of offshore storage potential in the US Exclusive Economic Zone. Greenh Gases: Sci Tech 2013;3(1):84–95.
[27] Jacobs W, Stump D. Proposed liability framework for geological sequestration of carbon dioxide; 2010.
[28] Wildenborg T, Bentham M, Chadwick A, David P, Deflandree J-P, Dillen M, et al. Large-scale CO_2 injection demos for the development of monitoring and verification technology and guidelines (CO_2 ReMoVe). Energy Proc 2009;1(1):2367–74.
[29] Aker E, Bjørnarå T, Braathen A, Brandvoll Ø, Dahle H, Nordbotten JM, et al. SUCCESS: SUbsurface CO_2 storage–Critical elements and superior strategy. Energy Proc 2011;4:6117–24.
[30] Taylor P, Lichtschlag A, Toberman M, Sayer MD, Reynolds A, Sato T, et al. Impact and recovery of pH in marine sediments subject to a temporary carbon dioxide leak. Int J Greenh Gas Control 2015;38:93–101.
[31] Langford R, Borissova I, Chirinos A, Henson P, Heap A. Pre-competitive data acquisition program for CO2 storage in australia. Energy Proc 2013;37:4968–74.
[32] Borissova I, Kennard J, Lech M, Wang L, Johnston S, Lewis C, et al. Integrated approach to CO_2 storage assessment in the offshore South Perth basin, Australia. Energy Proc 2013;37:4872–8.
[33] House KZ, Schrag DP, Harvey CF, Lackner KS. Permanent carbon dioxide storage in deep-sea sediments. Proc Natl Acad Sci USA 2006;103(33):12291–5.
[34] Schrag DP. Storage of carbon dioxide in offshore sediments. Science 2009;325(5948):1658–9.
[35] Levine JS, Matter JM, Goldberg D, Cook A, Lackner KS. Gravitational trapping of carbon dioxide in deep sea sediments: Permeability, buoyancy, and geomechanical analysis. Geophys Res Lett 34 (24), l24703. http://dx.doi.org/10.1029/2007GL031560.
[36] Fer I, Haugan PM. Dissolution from a liquid CO_2 lake disposed in the deep ocean. Limnol Oceanogr 2003;48(2):872–83.
[37] Koide H, Shindo Y, Tazaki Y, Iijima M, Ito K, Kimura N, et al. Deep sub-seabed disposal of CO_2 —the most protective storage—. Energ Convers Manage 1997;38:S253–8.
[38] Eccles JK, Pratson L. Global CO_2 storage potential of self-sealing marine sedimentary strata. Geophys Res Lett 39 (19).
[39] Soltanian MR, Amooie MA, Gershenzon N, Dai Z, Ritzi R, Xiong F, et al. Dissolution trapping of carbon dioxide in heterogeneous aquifers. Environ Sci Technol. http://dx.doi.org/10.1021/acs.est.7b01540.
[40] Dai Z, Viswanathan H, Middleton R, Pan F, Ampomah W, Yang C, et al. CO_2 accounting and risk analysis for CO_2 sequestration at enhanced oil recovery sites. Environ Sci Technol 2016;50(14):7546–54.
[41] Bacon D, Qafoku N, Dai Z, Keating E, Brown C. Modeling the impact of carbon dioxide leakage into an unconfined, oxidizing carbonate aquifer. Int J Greenh Gas Con 2016;44:290–9.
[42] Reece JS, Flemings PB, Dugan B, Long H, Germaine JT. Permeability-porosity relationships of shallow mudstones in the Ursa Basin, northern deepwater Gulf of Mexico. J Geophys Res Solid Earth 117 (B12).
[43] Boswell R, Shelander D, Lee M, Latham T, Collett T, Guerin G, et al. Occurrence of gas hydrate in Oligocene Frio sand: Alaminos Canyon Block 818: Northern Gulf of Mexico. Mar Pet Geol 2009;26(8):1499–512.
[44] Gay A, Takano Y, Gilhooly III W, Berndt C, Heeschen K, Suzuki N, et al. Geophysical and geochemical evidence of large scale fluid flow within shallow sediments in the eastern gulf of mexico, offshore louisiana. Geofluids 2011;11(1):34–47.
[45] Milkov AV, Sassen R. Estimate of gas hydrate resource, northwestern gulf of Mexico continental slope. Mar Geol 2001;179(1–2):71–83.
[46] Van Genuchten MT. A closed-form equation for predicting the hydraulic conductivity of unsaturated soils. Soil Sci Soc Am J 1980;44(5):892–8.
[47] Unver A, Himmelblau D. Diffusion coefficients of CO2, C2H4, C3H6 and C4H8 in water from 6 to 65 c. J Chem Eng Data 1964;9(3):428–31.
[48] Thomas W, Adams M. Measurement of the diffusion coefficients of carbon dioxide and nitrous oxide in water and aqueous solutions of glycerol. Trans Faraday Soc 1965;61:668–73.
[49] Zyvoloski GA, Robinson BA, Dash ZV, Trease LL. Summary of the models and methods for the fehm application-a finite-element heat-and mass-transfer code. Tech rep, Los Alamos National Lab., NM (US); 1997.
[50] Dai Z, Stauffer PH, Carey JW, Middleton RS, Lu Z, Jacobs JF, et al. Pre-site characterization risk analysis for commercial-scale carbon sequestration. Environ Sci Technol 2014;48(7):3908–15.
[51] Tong C. Psuade user's manual (version 1.2. 0). Tech. rep., Technical Report, LLNLSM-407882, Lawrence Livermore National Laboratory, Livermore, CA 94551-0808; 2011.
[52] Deutsch C, Journel A. GSLIB: Geostatistical Software Library and User's Guide, Applied geostatistical series, Oxford University Press; 1992. <https://books.google.com/books?id=BiZOAQAAIAAJ>.
[53] Divins D. Total sediment thickness of the World's Oceans & Marginal Seas, NOAA National Geophysical Data Center, Boulder, CO; 2003.
[54] Linstrom PJ, Mallard W. NIST Chemistry WebBook, NIST Standard Reference Database Number 69, National Institute of Standards and Technology, Gaithersburg MD, 20899; 2017.
[55] Soltanian MR, Amooie MA, Cole DR, Darrah TH, Graham DE, Pfiffner SM, et al. Impacts of methane on carbon dioxide storage in brine formations. Groundwater 56 (2).